

Simulation Studies of the Hydration Entropy of Simple, Hydrophobic Solutes

Themis Lazaridis† and Michael E. Paulaitis*

Center for Molecular and Engineering Thermodynamics, Department of Chemical Engineering, University of Delaware, Newark, Delaware 19716

Received: June 4, 1992*

The contribution of solute-water correlations to the entropy of solution of monatomic, hydrophobic solutes in water is calculated by Monte Carlo simulations using an expansion in terms of multiparticle correlation functions. The solute-water orientational correlations are found to decay linearly with intermolecular distance and virtually vanish in the second hydration shell. The results for the hydration entropies of inert gases, compared to experimental values, appear to be reasonable. The dependence of the entropy on the solute size and the solute-solvent pair interaction energy is examined by simulations of model Lennard-Jones particles in water. The primary factor determining the solute-water entropy is found to be solute size, with the pair interaction energy playing a secondary, but significant, role. The dependence of the orientational entropy on the curvature of the solute surface is discussed in connection with enthalpy-entropy compensation phenomena.

Introduction

In a recent publication (hereafter called LP) we presented a formulation for the entropy of solution of simple, monatomic solutes in water based on an expansion of the entropy in terms of multiparticle correlations.¹ The two-particle solute-water term was evaluated by Monte Carlo simulations for the case of methane at infinite dilution in water. It was found that methane-water translational and orientational pair correlations alone can account for the large negative entropies and the large positive heat capacities of hydration of hydrophobic molecules, at least at room temperature. The contribution of changes in water-water correlations upon solute insertion to the entropy was not calculated.² However, judging from the excellent correspondence between the solute-water terms and experimental data, this contribution appears to be small when solute insertion takes place at constant temperature and pressure.³

In this work we extend our simulation studies to the hydration of inert gases and model Lennard-Jones particles at infinite dilution in order to characterize the dependence of the hydration entropy on solute size and solute-solvent pair interaction energy. In addition, we examine two of the key assumptions in LP, namely the decoupling of translational and orientational correlations in the first hydration shell and the neglect of orientational correlations in the second and higher shells.

Theory and Simulation Method

In this section we briefly present the formulas for the multiparticle correlation function expansion of the entropy used in this work. Details of the derivation can be found in LP¹ and in a more recent communication.³

Neglecting intramolecular degrees of freedom, the entropy of a polyatomic fluid in the canonical ensemble can be expressed as follows:¹

$$S_N = -\frac{kN}{\rho} \frac{\Omega}{\sigma} \int f^{(1)}_N \ln(h^s f^{(1)}_N) \, d\mathbf{p}_1 \, d\mathbf{J}_1 - \frac{k\rho^2}{2\Omega^2} \int g^{(2)} \ln g^{(2)} \, d\mathbf{r}^2 \, d\omega^2$$

$$-\frac{k\rho^3}{3!\Omega^3} \int g^{(3)} \ln \delta g^{(3)} \, d\mathbf{r}^3 \, d\omega^3 - \dots \quad (1)$$

where k is Boltzmann's constant, h Planck's constant, ρ the number density (N/V), \mathbf{r}^N the Cartesian coordinates of the N molecules, \mathbf{p}^N the linear momenta, ω^N the Euler angles, \mathbf{J}^N the angular momenta, $\Omega = \int d\omega$, σ the symmetry number of the molecules (2 for water), s the number of external degrees of freedom per molecule (6 for nonlinear molecules), $f^{(1)}_N$ the one-particle distribution function, and $g^{(n)}$ the n -particle correlation function. The quantity $\delta g^{(3)}$ is defined by

$$g^{(3)}(1,2,3) = g^{(2)}(1,2) g^{(2)}(1,3) g^{(2)}(2,3) \delta g^{(3)}(1,2,3) \quad (2)$$

and similarly for $\delta g^{(n)}$, $n = 4, \dots, N$. The above expression is derived by a Kirkwood factorization of the N -particle correlation function and substitution into the Gibbs expression for the entropy.⁴ The first term, the one-particle contribution, reflects the ability of each particle to visit any point in the volume of the system. The second term accounts for correlations in the positions and orientations of the molecules, while the higher order terms represent correlations that cannot be accounted for by the superposition approximation ($\delta g^{(3)} = 1$ in eq 2).

The entropy of a mixture can be similarly expressed in terms of multiparticle correlation functions. In the case of an aqueous mixture of a monatomic solute the expression for the entropy is

$$S = N_w \left(\frac{6}{2}k - k \ln(\rho_w \Lambda_w^3 q_w^{-1}) \right) + N_s \left(\frac{3}{2}k - k \ln(\rho_s \Lambda_s^3) \right) - N_w^2 \frac{k}{2V\Omega^2} \int g_{ww} \ln g_{ww} \, d\mathbf{r} \, d\omega^2 - N_s^2 \frac{k}{2V} \int g_{ss} \ln g_{ss} \, d\mathbf{r} - N_s N_w \frac{k}{V\Omega} \int g_{sw} \ln g_{sw} \, d\mathbf{r} \, d\omega + \text{higher order terms} \quad (3)$$

where subscripts s and w denote solute and water, respectively, N_w and N_s are the number of molecules, ρ_w and ρ_s are number densities, q_w is the rotational partition function of water, and g_{ww} , g_{sw} , and g_{ss} are pair correlation functions.

The partial molar entropy of the solute is obtained by differentiating eq 3 with respect to N_s at constant T , P , and N_w . At infinite dilution this partial molar entropy is given by

$$\bar{S}_s^\infty = \left(\frac{3}{2}k - k \ln(\rho_s \Lambda_s^3) \right) - k(1 - \rho_w \bar{v}_s^\infty) - k \frac{\rho_w}{\Omega} \int g_{sw} \ln g_{sw} \, d\mathbf{r} \, d\omega +$$

* Author to whom correspondence should be addressed.

† Present address: Department of Chemistry, Harvard University, Cambridge, MA 02138.

• Abstract published in *Advance ACS Abstracts*, November 15, 1993.

$$\frac{k\rho_w^2}{2\Omega^2} \int_{\infty}^{\infty} g_{ww} \ln g_{ww} dr d\omega^2 - \frac{k\rho_w}{2\Omega^2} \times \left(\frac{\partial}{\partial x_s} \int g_{ww} \ln g_{ww} dr d\omega^2 \right)_{T,P} + \text{higher order terms} \quad (4)$$

The term $k(1 - \rho_w \bar{v}_s^{\infty})$ arises from the derivative of the first two terms in eq 3, and we will refer to this term as the "volume entropy".⁵

The terms involving the water-water correlation function account for "solvent reorganization" upon solute insertion. The calculation of these terms, as well as of the higher order terms, is very difficult to perform by simulation. Our results in LP suggest that these terms must be small at room temperature. Therefore, in what follows we concentrate on the two-particle solute-water term, which can be expressed as

$$S_{sw} = - \frac{k(N-1)}{V\Omega} \int g_{sw}^{(2)} \ln g_{sw}^{(2)} dr d\omega \quad (5)$$

By performing the following factorization of the pair correlation function¹

$$g_{sw}^{(2)}(r, \theta, \phi, \chi) = g_{sw}^r(r) g(\theta, \chi, \phi) \quad \text{for } r \leq r_{sh} \quad (6)$$

$$g_{sw}^{(2)}(r, \theta, \phi, \chi) = g_{sw}^r(r) \quad \text{for } r \geq r_{sh}$$

where g_{sw}^r is the orientationally averaged radial distribution function (RDF) and r_{sh} is defined as the distance to its first minimum, we can separate the residual entropy into a translational and an orientational contribution:

$$S_{sw} = - \frac{k(N-1)}{V} \int g_{sw}^r \ln g_{sw}^r dr \quad (\text{translational})$$

$$- \frac{k(N-1)V_i}{V\Omega} \int g(\theta, \chi, \phi) \ln\{g(\theta, \chi, \phi)\} d\omega \quad (\text{orientational}) \quad (7)$$

For spherically symmetric solutes, the orientational correlation function will be uniform with respect to the third Euler angle, ϕ . The angle θ is defined as that between the dipole vector of water and the solute-water oxygen axis, while χ describes rotation around the water dipole vector (see Figure 1 of LP).

The first integral in eq 7 runs over the entire volume of the fluid. However, in simulations g_{sw}^r can only be calculated up to a certain distance, usually less than 15 Å. This is not a problem if this RDF is short-ranged—i.e., exactly unity at longer separations. In LP we calculated g_{sw}^r up to 8 Å and assumed that it takes the value 1 at longer separations. We then scaled the calculated RDF to ensure that

$$\int_0^8 g_{sw}^r dr_1 = \int_0^8 dr_1$$

which arises from the normalization condition,

$$\int g_{sw}^r dr_1 = V \quad (8)$$

where the integration is over the entire volume of the fluid. (This is implied hereafter when no integration limits are given.) With the new simulation results we have examined the ratio $\int_0^R dr / \int_0^R g_{sw}^r dr$ where R is the cutoff distance for the RDF and found that this ratio varies systematically with solute size. It is slightly less than 1 for the point cavities and gradually increases to values greater than 1 for larger solutes. We believe there are two effects that lead to this behavior:

(a) The solute introduces in the solvent a local density enhancement that decays gradually with distance from the solute. This decay may not be complete at the point where the RDF is truncated, and this will tend to make the above ratio less than 1.

(b) The solute excludes solvent molecules from the volume it occupies. Therefore, the overall density of the solvent in any sphere around the solute is smaller than in regions of pure solvent by the mere fact that this sphere contains the solute. This effect increases with solute size and tends to make the above ratio greater than 1.

Thus, it follows that g_{sw}^r will not become exactly 1 at any distance from the solute. In other words, even though the normalization condition in eq 8 holds, the first integral in eq 7 is not truly "local"⁶ and consideration must be given to the behavior of the RDF at longer distances. A simple analysis of this long-range behavior is given below.

Consider the calculation of the RDF up to some arbitrary distance R and let $\int_0^R g_{sw}^r dr = V_0$. Since we do not know the behavior of g_{sw}^r at longer distances, we assume that it is constant and equal to g_1 between R and another distance R_1 , after which it becomes equal to unity. The correction to the calculated entropy due to this long-range behavior of g_{sw}^r will be

$$S_{\text{corr}} = -k\rho_w \int_R^{R_1} g_{sw}^r \ln g_{sw}^r dr = -k\rho_w g_1 \ln g_1 (V_1 - V_R) \quad (9)$$

where $V_1 = 4/3\pi R_1^3$ and $V_R = 4/3\pi R^3$. From the normalization condition, $\int g_{sw}^r dr = V$, we find that g_1 must be equal to $(V_1 - V_0)/(V_1 - V_R)$. There is still uncertainty as to the value of R_1 ; however, eq 9 turns out to be rather insensitive to this value. In fact, if we take the limit $R_1 \rightarrow \infty$, we arrive at the simple expression

$$S_{\text{corr}} = -k\rho_w (V_R - V_0) = k\rho \int_0^R (g_{sw}^r - 1) dr \quad (10)$$

For a pure fluid in the canonical ensemble, where the normalization condition is $\int g^{(2)} dr = V(1 - 1/N)$, the above procedure will give an entropy correction

$$S_{\text{corr}} = k \int_0^R (g^r - 1) dr + \frac{1}{2}k \quad (11)$$

Wallace has apparently used a similar long-range correction to calculate the entropy for the hard-sphere fluid at high densities.⁴ These terms also arise in an alternate expansion of the entropy derived by Baranyai and Evans.⁶ For a pure, monatomic fluid this expansion is

$$\frac{S_N}{N} = - \frac{k}{\rho} \int f^{(1)} \ln(h^3 f^{(1)}) dp_1 - \frac{k\rho}{2} \int g^{(2)} \ln g^{(2)} dr + \frac{1}{2}k + \frac{k\rho}{2} \int (g^{(2)} - 1) dr - \frac{k\rho^2}{3!} \int g^{(3)} \ln \delta g^{(3)} dr^2 + \frac{1}{6}k + \frac{k\rho^2}{3!} \int (g^{(3)} - 3g^{(2)}g^{(2)} + 3g^{(2)} - 1) dr^2 - \dots \quad (12)$$

where the series $1/2k, 1/6k, \dots$ sums to k and, when added to the one-particle term, is equal to the entropy of an ideal monatomic gas: $5/2 - k \ln(\rho \Lambda^3)$. The above expression, which these authors showed holds in the canonical ensemble, is identical to the correlation function expansion of the entropy in the grand canonical ensemble.^{7,8} The third and fourth terms in this expansion, which are identical to eq 11, cancel each other in the canonical ensemble when the integration is performed over the entire volume. However, when the integration is cut off at a finite distance, our analysis shows that these terms give the correction due to the omitted long-range behavior of the RDF, supporting the argument that eq 12 is local and therefore should be more accurate for numerical calculations.

In this work we employ the long-range correction of eq 10. We have found, though, that the values for the entropy calculated by this procedure are virtually identical (within statistical uncertainty) to those obtained by our previous practice of scaling the RDF. That is, when the solute is about the same size as the

solvent, this correction was found to be very small, but it can become comparable to the $g_{sw}^r \ln g_{sw}^r$ integral in eq 7 for large solutes.

To compare with experiment, we need to establish the connection between the partial molar entropy (eq 4) and the reported standard entropies of solvation. Ben-Naim's standard solvation entropy is defined as the temperature-derivative of the residual chemical potential⁹

$$\Delta S_s^* = -\frac{\partial \mu_s^{\text{res}}}{\partial T} \quad (13)$$

where

$$\mu_s^{\text{res}} = \mu_s - kT \ln(\rho_s \Lambda_s^3) \quad (14)$$

The partial molar entropy is

$$\begin{aligned} \bar{S}_s &= -\frac{\partial \mu_s}{\partial T} = -\frac{\partial \mu_s^{\text{res}}}{\partial T} - k \ln(\rho_s \Lambda_s^3) + kT\alpha + \frac{3}{2}k \\ &= \Delta S_s^* - k \ln(\rho_s \Lambda_s^3) + kT\alpha + \frac{3}{2}k \end{aligned} \quad (15)$$

where α is the thermal expansion coefficient of the solution. Equation 15, when compared to eq 4 gives, at infinite dilution,

$$\begin{aligned} \Delta S_s^{*\infty} &= -kT\alpha^\circ - k(1 - \rho_w \bar{v}_s^\infty) - \frac{k(N-1)}{V} \int g_{sw}^r \ln g_{sw}^r dr \\ &\quad - \frac{k(N-1)V_i}{V\Omega} \int g(\theta, \chi, \phi) \ln\{g(\theta, \chi, \phi)\} d\omega + \dots \end{aligned} \quad (16)$$

where α° is the thermal expansion coefficient of water.

The RDF and the orientational distribution function are calculated by Monte Carlo simulation using Jorgensen's BOSS program.¹⁰ For these simulations one particle is inserted in a box of 216 water molecules pre-equilibrated at 25 °C. Then, depending on solute size, one or two water molecules exhibiting the highest interaction energy with the solute are deleted to approximate particle dissolution at constant pressure. NVT simulations for the mixture are then performed at 25 °C. Pre-equilibration of the mixture at a constant pressure of one atmosphere was not considered necessary, since in LP it was found that NPT and NVT simulations gave similar results for the calculated entropy. Each simulation consisted of 5 million or more configurations for equilibration and from 20 to 60 million configurations for sampling. The TIP4P model for water¹¹ was used in all simulations. The solute-water pair correlation entropy was calculated from eq 7 with the RDF numerically integrated up to 8 Å for the smaller solutes and up to 10.5 Å for the larger ones. The orientational distribution function was numerically integrated as described in LP.

Distance Dependence of Orientational Correlations

Equation 6 assumes that the orientational distribution function is independent of distance within the first hydration shell and that it is uniform in the second and higher shells. These assumptions are tested here for methane in water by calculating the orientational distribution function in three subshells of the first hydration shell as well as in the second hydration shell. The first subshell extends up to 3.8 Å, the second between 3.8 and 4.6 Å, and the third between 4.6 and 5.4 Å. The second hydration shell extends from 5.4 to 7.4 Å (see Figure 1). The Lennard-Jones parameters used for methane are the same as in LP ($\sigma = 3.73$ Å and $\epsilon = 0.294$ kcal/mol).

Since the subshell calculations demand better statistics than a calculation sampling over the whole first hydration shell, the simulation was extended to 100 million configurations. Contour plots of the orientational distribution function in the three subshells

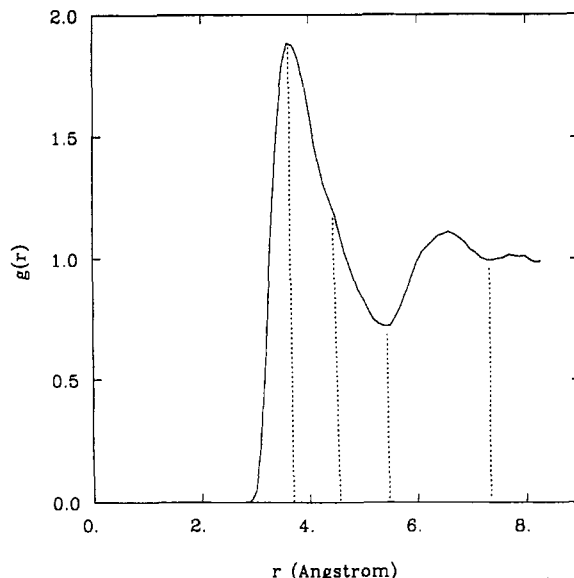


Figure 1. Methane-water oxygen radial distribution function. Vertical lines show the separation into subshells and the second hydration shell.

of the first hydration shell and in the second hydration shell are shown in Figure 2. Consistent with previous simulation work,¹² the orientational distribution in the three subshells is qualitatively similar; only in the third subshell do we observe a shift in the position of the maxima (denoted by plus signs in Figure 2). However, the distribution becomes progressively less pronounced with increasing distance from the solute. In the second hydration shell the distribution is more nearly uniform, although some very weak orientational preferences are still evident. Notably, these orientational preferences are opposite to those in the first shell; i.e., on average, water molecules in the second shell tend to point one of their tetrahedral bonding vectors toward the solute, apparently to form hydrogen bonds with the water molecules in the first shell, which are oriented in the opposite direction.

The second integral in eq 7, divided by Ω , gives the orientational entropy per water molecule and is a good measure of the extent of orientational correlations. This quantity is plotted in Figure 3, where it is observed to decay almost linearly with distance from the solute. The total orientational contribution to the hydration entropy per methane molecule is given by a sum of terms identical to those in eq 7, one term for each hydration shell or subshell, where $(N-1)V_i/V$ is replaced by the average number of water molecules in that shell or subshell. The average number of water molecules is 5.6 in the first hydration subshell, 8 in the second, 7 in the third, and 25.7 in the second hydration shell. These contributions to the orientational entropy are -3.2 , -3.4 , -1.3 , and -0.7 eu, respectively, bringing the total to -8.6 eu. This value is more negative than that obtained from our previous calculation¹ (-6.6 eu) but is in reasonable agreement given the statistical uncertainties inherent in this approach for calculating the entropy. It should be noted that orientational correlations are almost nonexistent beyond the first hydration shell and thus appear to make a very small contribution to the entropy. This is consistent with neutron and X-ray diffraction measurements¹³ for pure water showing that orientational correlations decay much faster than positional correlations.

Therefore, while the assumption of decoupled orientational and translational correlations (eq 6) is not strictly correct, the results obtained on the basis of this assumption are quite close to those obtained through the present more rigorous (and laborious!) calculation. The reason is that the orientational distribution is qualitatively the same throughout the first hydration shell. If that were not the case and we sampled over regions with opposite orientational preferences, the magnitude of the entropy would be significantly underestimated. Since the computational require-

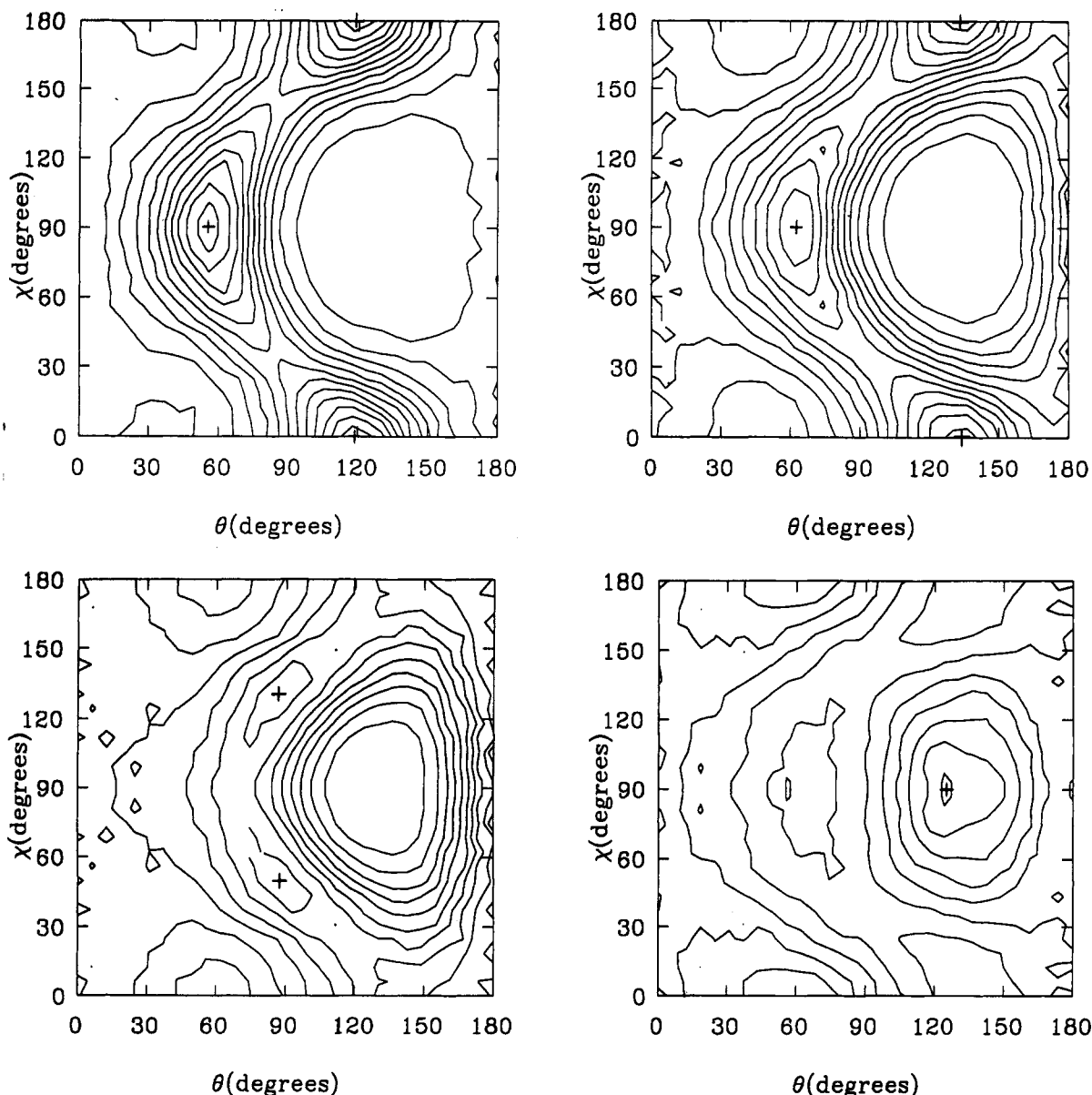


Figure 2. Contour plots of the orientational distribution function of water molecules in the first (top left), second (top right), and third (bottom left) subshells and in the second hydration shell (bottom right).

ments of performing rigorous subshell calculations are quite large, it will be expedient to continue to apply eq 6, knowing, though, that this approximation may impose a limitation of 1 or 2 eu in the accuracy we can achieve by this method. In doing so in the present study, we assume that the variation of orientational correlations with distance from solutes of different size is qualitatively similar to that observed for methane.

Hydration of Inert Gases

The inert gases are modeled as Lennard-Jones particles with the parameters listed in Table I. The calculated sum of the four terms in eq 16 is reported in Table II and compared to experimental data. These calculations are based on a total of 60 million configurations for each system. Partial molar volumes have not been calculated from these simulations, although methods for doing so have been proposed in the literature.¹⁴ To obtain the volume entropy term, we use the experimental partial molar volume of argon¹⁵ and estimate the partial molar volumes of the remaining gases from a corresponding states correlation based on Kirkwood-Buff solution theory.¹⁶ We take the characteristic volume in this correlation to be the atomic volume ($\pi\sigma^3/6$) for all the gases. For the $kT\alpha^\circ$ term, the experimental thermal

expansion coefficient of water is used ($\alpha^\circ = 257.21 \times 10^{-6} \text{ K}^{-1}$).¹⁷ From Table II it can be seen that the sum of the calculated contributions to the entropy agrees quite well with experimental values. However, we cannot place too much significance in this agreement in view of the approximations involved in obtaining these estimates. Also, there is some uncertainty in the Lennard-Jones parameters used. Other simulation work¹⁸ employed significantly larger size parameters for helium and neon (2.9 and 3.1 Å, respectively). Difficulties in reproducing the value and temperature dependence of experimental solubilities for helium and neon using common values of the Lennard-Jones parameters were also encountered in the work of Swope and Andersen.¹⁹ With regard to radon, this gas has not been frequently studied and its Lennard-Jones parameters, derived theoretically, are not completely consistent with experimental data.²⁰ Overall, the results appear to be reasonable, reproducing the observed increase in the magnitude of the hydration entropy with increasing size of the molecule. It would be interesting to compare these results with calculations based on other molecular theories, such as the theory of Pratt and Chandler.²¹ This will be reported in a future publication.

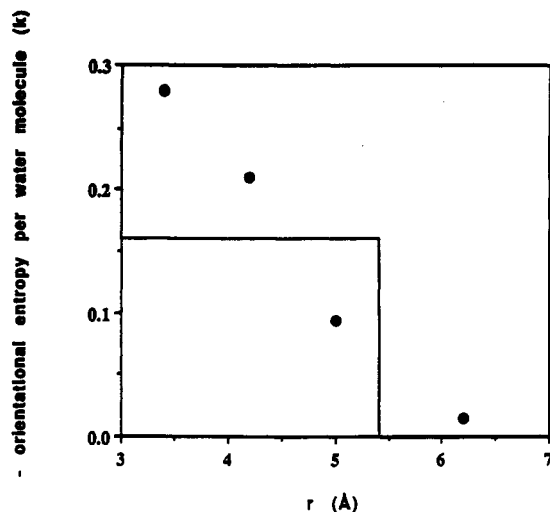


Figure 3. Orientational entropy per water molecule (in units of Boltzmann's constant) in three subshells of the first hydration shell and in the second hydration shell. (The solid line corresponds to the calculation based on the assumption in eq 6.)

TABLE I: Lennard-Jones Parameters for the Inert Gases

	$\sigma(\text{\AA})$	ϵ (kcal/mol)
helium ^a	2.55	0.02
neon ^a	2.78	0.069
argon ^b	3.401	0.2339
krypton ^b	3.624	0.317
xenon ^b	3.935	0.433
radon ^c	4.36	0.576

^a Hirschfelder, J. O.; Curtiss, C. F.; Bird, R. B. *Molecular Theory of Gases and Liquids*; Wiley: New York, 1954. ^b Verlet, L.; Weis, J.-J. *Mol. Phys.* 1972, 24, 1013. ^c Miller, G. A. *J. Phys. Chem.* 1960, 64, 163.

TABLE II: Simulation Results for the Hydration Entropy of Inert Gases at 25 °C^a

	transl correl	orient. correl	vol entropy contribution	tot calcd	exptl ^b	
helium	-4.6	-3.0	+0.1	-7.7	-8.0,	-7.8
neon	-6.2	-4.1	+0.5	-10.0	-10.1, -10.8,	-10.0
argon	-10.5	-6.2	+1.5	-15.4	-14.7, -15.6,	-14.4
krypton	-11.4	-7.0	+2.0	-16.5	-16.3, -16.8,	-16.0
xenon	-13.4	-7.3	+2.6	-18.3	-17.4, -19.6,	-17.8
radon	-16.0	-8.6	+3.5	-21.3	-18.2	

^a All values in eu (1 eu = 1 cal/mol·K). The $kT\alpha^\circ$ term is included in the total calculated entropy. ^b First and second columns from: Ben-Naim, A. *Solvation Thermodynamics*; Plenum: New York, 1987. Third column from: Krause, D., Jr.; Benson, B. B. *J. Solution Chem.* 1989, 18, 823 (after change of standard states).

Dependence of the Entropy on Size and Interaction Energy

The calculated results for the inert gases show substantial differences in the entropy of hydration, depending on the solute. However, the data cannot reveal whether the variation is due to the size of the solute or to the solute-water interaction energy. In this section we study a number of model Lennard-Jones solutes in water, varying separately the interaction energy and the size of the solute.

Figure 4 shows plots of the Lennard-Jones potential for one value of σ but different values of ϵ . From this picture it is clear that σ (i.e., the intermolecular distance where the interaction energy is zero) is not a good measure of molecular size. We use instead the thermal diameter σ_{th} for solute-water interactions, defined as the intermolecular distance where the interaction energy is equal to the thermal energy (0.6 kcal/mol at 300 K). With a very small ϵ , the Lennard-Jones potential will closely emulate a hard-sphere potential. These simulations of purely repulsive solutes are performed to facilitate a comparison of the present method with analytical theories, such as the scaled particle theory.

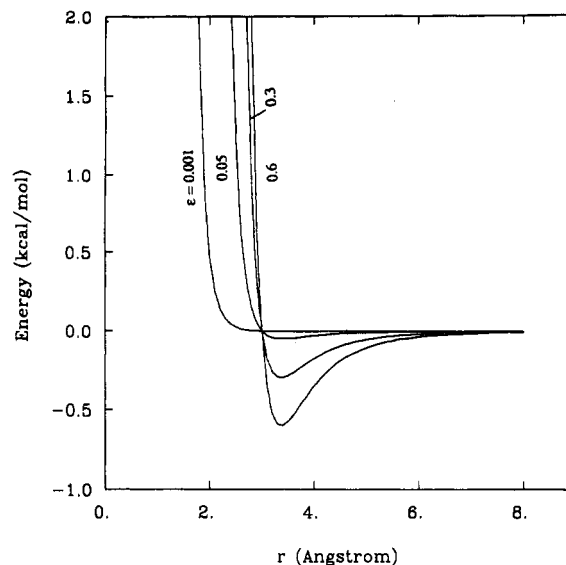


Figure 4. Lennard-Jones potentials at $\sigma = 3 \text{ \AA}$ and four different values of ϵ .

The BOSS program uses the geometric mean, combining rules for the Lennard-Jones parameters characterizing solute-water interactions,

$$\epsilon = \sqrt{\epsilon_s \epsilon_w}$$

$$\sigma = \sqrt{\sigma_s \sigma_w}$$

where the subscripts s and w stand for the solute and water, respectively. The values for TIP4P water are $\epsilon_w = 0.1521 \text{ kcal/mol}$ and $\sigma_w = 3.15061 \text{ \AA}$. The thermal diameter σ_{th} for solute-water interactions is defined by

$$4\epsilon \left[\left(\frac{\sigma}{\sigma_{th}} \right)^{12} - \left(\frac{\sigma}{\sigma_{th}} \right)^6 \right] = kT$$

and the effective solute diameter is defined as

$$\sigma_s^{eff} = 2\sigma_{th} - \sigma_w$$

Table III lists the model solutes studied. The first four systems emulate a point cavity with different values of the interaction energy. Similarly for the next six systems which, in this case, are for a solute of finite size. The remaining systems correspond to purely repulsive solutes of different size. The translational and orientational correlation terms in eq 16 were calculated and are reported in Table III. The volume entropy term was not calculated. This term will make a positive contribution to the entropy for solutes with partial molar volumes greater than the molar volume of water, and a negative contribution in the opposite case. The results in Table III and Figures 5-8 reveal that the size of the solute is the dominating factor in determining both the translational and orientational correlation entropies, with the solute-water interaction energy playing a less significant role. Figure 5 shows a rapid increase in the magnitude of the translational correlation entropy with increasing effective solute diameter. This effect can be rationalized by a free volume argument:²² as the size of the solute increases (or the size of the solvent decreases), the solvent molecules can pack around the solute more effectively. This restricts the translational freedom of the solute, since any motion of the solute must occur in concert with the motion of a large number of solvent molecules. The upward curvature in Figure 5 is characteristic of analogous curves for the entropy or the free energy of cavity formation as a function of cavity size obtained by scaled particle theory^{23,24} and in computer simulations.^{23,25} The translational correlation entropy is negative for all solutes as expected. For comparison, scaled particle theory predicts a small, negative value (-0.8 eu) for the entropy of solution of a point cavity in water.²⁶

TABLE III: Lennard-Jones Systems Studied and Results Obtained^a

σ_s	ϵ_s	ϵ	σ_{th}	σ_s^{eff}	transl correl S	orient correl S per water molecule	N_c
1.252	0.001	0.012 33	1.575	0.0	-1.1	-0.082	7.4
0.962	0.066	0.1	1.575	0.0	-1.3	-0.084	5.3
0.901	0.263	0.2	1.575	0.0	-1.5	-0.132	5.3
0.874	0.592	0.3	1.575	0.0	-1.7	-0.120	7.6
4.773	0.001	0.012 33	3.075	3.0	-8.4	-0.310	19.2
3.667	0.066	0.1	3.075	3.0	-9.5	-0.320	18.2
3.435	0.263	0.2	3.075	3.0	-10.5	-0.366	19.6
3.330	0.592	0.3	3.075	3.0	-11.2	-0.388	19.9
3.266	1.052	0.4	3.075	3.0	-11.8	-0.340	18.7
3.226	1.644	0.5	3.075	3.0	-12.3	-0.360	19.4
2.019	0.001	0.012 33	2.0	0.85	-2.3	-0.150	9.5
3.155	0.001	0.012 33	2.5	1.85	-4.6	-0.214	13
6.184	0.001	0.012 33	3.5	3.85	-12.2	-0.374	23
8.078	0.001	0.012 33	4.0	4.85	-16.7	-0.316	28
10.222	0.001	0.012 33	4.5	5.85	-23.6	-0.350	35
12.622	0.001	0.012 33	5.0	6.85	-31.1	-0.306	42
15.269	0.001	0.012 33	5.5	7.85	-41.5	-0.322	51
18.174	0.001	0.012 33	6.0	8.85	-52.5	-0.272	58.5

^a The units are Å for σ , kcal/mol for ϵ , and entropy units (cal/mol·K) for the entropies. N_c is the number of water molecules in the first hydration shell.

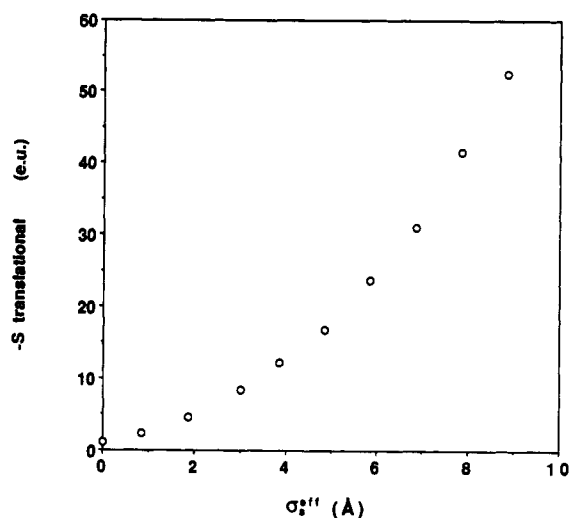


Figure 5. Translational correlation entropy of the Lennard-Jones particles as a function of effective solute diameter.

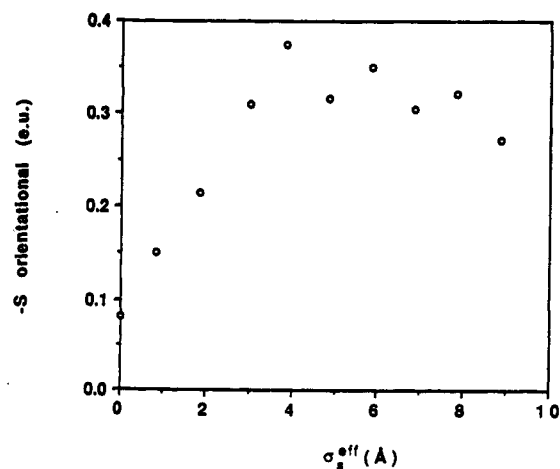


Figure 6. Orientational correlation entropy per water molecule as a function of effective solute diameter.

The orientational correlation entropy depends on the solute-water orientational correlations and the number of water molecules in the first hydration shell. As the solute size increases, this number increases as well. To separate out this effect, we plot in Figure 6 the orientational correlation entropy per water molecule in the first hydration shell as a function of solute size. The

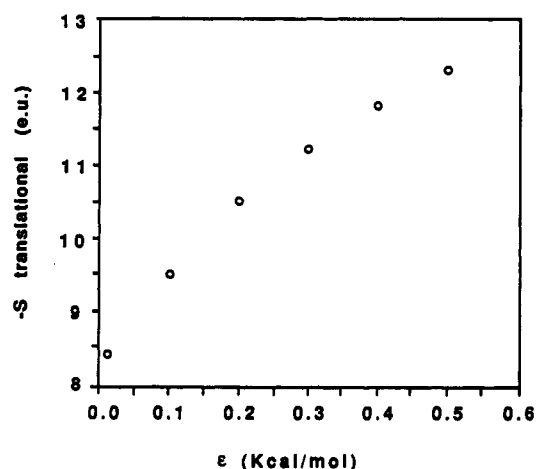


Figure 7. Translational correlation entropy as a function of interaction energy parameter for $\sigma_s^{eff} = 3$ Å.

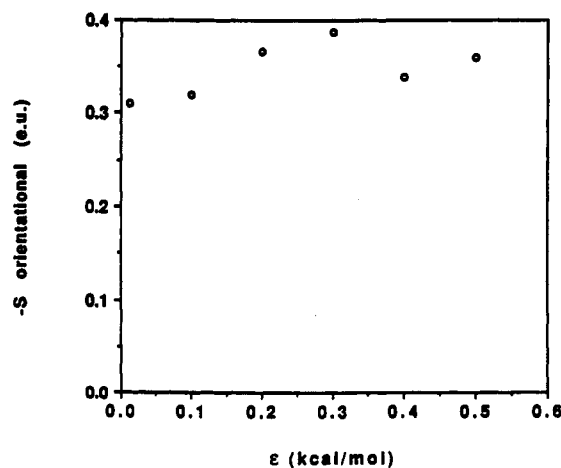


Figure 8. Orientational correlation entropy per water molecule as a function of interaction energy parameter for $\sigma_s^{eff} = 3$ Å.

magnitude of this quantity increases with solute size up to approximately 4 Å and then decreases slightly for larger solutes. Although there is some statistical noise in the data, this trend is clear.

The initial increase and subsequent decrease in the magnitude of the orientational correlations can be understood as follows. In the limit of a point cavity, water molecules are positionally restricted but orientationally free to form hydrogen bonds in all

directions. Thus, one would expect the magnitude of the orientational entropy in this limit to approach zero. However, orientational preferences qualitatively similar to those next to larger solutes are still observed next to point cavities, which may be due to the fact that even a point cavity induces a specific density pattern in the solvent around it. In addition, the calculated orientational distribution is an average over the entire first hydration shell and not exactly the distribution at the cavity-water contact distance. As the solute size increases and the curvature of its surface decreases, water molecules are forced to adopt more restricted orientations in order to form the maximum number of hydrogen bonds. As the curvature decreases further, water molecules near the surface are not able to form four linear hydrogen bonds no matter how they orient. Thus the energetic advantage of "straddling" configurations is diminished, and the orientational configurational space for water molecules around the solute becomes more uniform energetically. This leads to a broadened orientational distribution and a higher (less negative) orientational entropy. An interesting connection can be made to simulations of water next to a hydrophobic surface,²⁷ where it was found that water molecules tend to point one of their hydrogens or lone pairs toward the surface, thus sacrificing on average one hydrogen bond. Apparently this configuration becomes energetically favored over the "straddling" configuration next to a flat surface. It follows that the magnitude of the orientational entropy may exhibit a minimum with respect to surface curvature at the point where these two configurations become energetically equivalent.

Figures 7 and 8 show the variation of the translational and orientational entropies of hydration as a function of the interaction energy parameter for the 3-Å solutes in Table III. The results are qualitatively similar for the point solutes. The effect of ϵ on the orientational entropy is small and appears level over the entire range of ϵ . The effect on the translational entropy is more substantial but much smaller than that for solute sizes over the usual range of Lennard-Jones parameters for small solutes. The increase in the magnitude of the translational entropy with ϵ is not difficult to understand, since stronger solute-water interactions naturally lead to more sharply peaked correlations. These results clearly show a significant entropic effect associated with turning on solute-solvent interactions that can lead to contributions of up to 4 eu in the hydration entropy.

Discussion

The analysis of orientational correlations in the various hydration subshells and the entropy calculations for the inert gases further support our viewpoint that the essential thermodynamics of hydrophobic hydration is accounted for by the pairwise translational and orientational correlations between the solute and the water molecules of hydration. The simulations of model Lennard-Jones particles demonstrate that the solute-water entropy is primarily determined by the solute size. However, the effect of the solute-water interaction energy cannot be neglected.

One of the most interesting findings of the present work is that the magnitude of the orientational entropy per water molecule in the first hydration shell exhibits a maximum at an effective solute diameter of 4 Å. Differences in the characteristics of hydration of small solutes versus flat hydrophobic surfaces have long been recognized.²⁷ However, the thermodynamic consequences of these differences have not been examined in detail. The sacrifice of a hydrogen bond next to a flat surface will necessarily manifest itself thermodynamically in an increase in the enthalpic cost of the interaction. This may be one reason for the observation of enthalpy-driven association processes in water.^{28,29} While the enthalpy must become progressively more positive with decreasing surface curvature, the entropy probably changes in a more complex way. It is unknown, however, how the net free energy of the interaction will change with surface

curvature. If we accept that the reorientational relaxation of water to a state of lower entropy and energy is accompanied by a favorable free energy (which should be true, since this process occurs spontaneously next to small solutes at room temperature), it is natural to hypothesize that when this process cannot occur (e.g., next to a flat surface), the free energy will be higher.

This picture of hydrophobic hydration is in qualitative agreement with an empirical geometric model proposed recently for the dependence of the hydrophobic free energy on the curvature of the solute-water interface.^{30,31} In this model it is assumed that the free energy is proportional to the solvent accessible surface of water molecules in the hydration shell of the solute. It is hoped that the present work will help provide a quantitative, molecular foundation to such methods.

An immediate goal for future research should be the extension of these simulation studies to flat and concave surfaces in order to fully characterize the dependence of the orientational entropy on surface curvature. However, entropy changes are only one aspect of the hydrophobic effect. It is also imperative to know how the enthalpy of solution is affected by the size of the solute and its interaction with the solvent. Therefore, accurate methods for the calculation of enthalpies of solution and interfacial energies in aqueous systems should be devised. Another major goal should be the development of a formal treatment of enthalpy-entropy compensation phenomena as a function of both temperature and geometrical parameters, such as surface curvature. Some work has been done on this subject in the past,^{32,33} but the issue is still rather obscure.

Extension of the present method of calculating the entropy to more complex systems, such as molecular, polar, or ionic solutes, is highly desirable but not trivial. For instance, in the case of ions, the perturbation of water-water correlations next to the ion is significant and must be taken into account in the entropy calculation. However, water-water correlation functions will be of higher dimensionality than those for the monatomic, uncharged solutes studied here and cannot be obtained easily by simulation unless inordinately long running times are employed. The study of these systems will probably require thoughtful approximations and perhaps some mathematical ingenuity.

Acknowledgment. Prof. W. L. Jorgensen is gratefully acknowledged for making the program BOSS available to us. We also thank Prof. R. H. Wood for numerous helpful discussions. This work was supported by the National Science Foundation (Grant CPE8351228). Partial support was also provided by Union Carbide, Merck, and Exxon.

References and Notes

- (1) Lazaridis, T.; Paulaitis, M. E. *J. Phys. Chem.* **1992**, *96*, 3847.
- (2) Smith, D. E.; Laird, B. B.; Haymet, A. D. J. *J. Phys. Chem.* **1993**, *97*, 5788.
- (3) Lazaridis, T.; Paulaitis, M. E. *J. Phys. Chem.* **1993**, *97*, 5789.
- (4) (a) Wallace, D. C. *J. Chem. Phys.* **1987**, *87*, 2282. (b) Wallace, D. C. *Phys. Rev. A* **1989**, *39*, 4843.
- (5) Sharp, K. A.; Nicholls, A.; Friedman, R.; Honig, B. *Biochemistry* **1991**, *30*, 9686.
- (6) (a) Baranyai, A.; Evans, D. J. *Phys. Rev. A* **1989**, *40*, 3817. (b) Wallace, D. C. *Phys. Rev. A* **1989**, *39*, 4843.
- (7) Nettleton, R. E.; Green, M. S. *J. Chem. Phys.* **1958**, *29*, 1365.
- (8) Raveché, H. J. *J. Chem. Phys.* **1971**, *55*, 2242.
- (9) Ben-Naim, A. *J. Phys. Chem.* **1978**, *82*, 792.
- (10) Jorgensen, W. L. BOSS version 2.8; Yale University: New Haven, CT, 1989.
- (11) Jorgensen, W. L.; Chandrasekhar, J.; Madura, J. D.; Impey, R. W.; Klein, M. L. *J. Chem. Phys.* **1983**, *79*, 926.
- (12) Zichi, D. A.; Rosky, P. J. *J. Chem. Phys.* **1985**, *83*, 797.
- (13) Narten, A. H. *J. Chem. Phys.* **1972**, *56*, 5681.
- (14) Debenedetti, P. *Mol. Simul.* **1989**, *2*, 33.
- (15) Toppel, E. W.; Gubbins, K. E. *J. Phys. Chem.* **1972**, *76*, 3044.
- (16) Brelvi, S. W.; O'Connell, J. P. *AIChE J.* **1972**, *18*, 1239.
- (17) *CRC Handbook of Chemistry and Physics*, 64th ed.; CRC Press: Boca Raton, FL, 1983.
- (18) Straatsma, T. P.; Berendsen, H. J. C.; Postma, J. P. M. *J. Chem. Phys.* **1986**, *85*, 6720.

- (19) Swope, W. C.; Andersen, H. C. *J. Phys. Chem.* **1984**, *88*, 6548.
(20) Miller, G. A. *J. Phys. Chem.* **1960**, *64*, 163.
(21) Pratt, L. C.; Chandler, D. *J. Chem. Phys.* **1977**, *67*, 3683.
(22) Lee, B. *J. Phys. Chem.* **1983**, *87*, 112.
(23) Postma, J. P. M.; Berendsen, H. J. C.; Haak, J. R. *Faraday Symp. Chem. Soc.* **1982**, *17*, 55.
(24) Lucas, M. *J. Phys. Chem.* **1976**, *80*, 359.
(25) Pohorille, A.; Pratt, L. C. *J. Am. Chem. Soc.* **1990**, *112*, 5066.
(26) Pierotti, R. A. *J. Phys. Chem.* **1965**, *69*, 281.
(27) Lee, C. Y.; McCammon, J. A.; Rossky, P. J. *J. Chem. Phys.* **1984**, *80*, 4448.
(28) Hinz, H.-J. *Annu. Rev. Biophys. Bioeng.* **1983**, *12*, 285.
(29) Smithrud, D. B.; Wyman, T. B.; Diederich, F. *J. Am. Chem. Soc.* **1991**, *113*, 5420.
(30) Sharp, K. A.; Nicholls, A.; Fine, R. F.; Honig, B. *Science* **1991**, *252*, 106.
(31) Nicholls, A.; Sharp, K. A.; Honig, B. *Proteins* **1991**, *11*, 281.
(32) Benzinger, T. H. *Nature* **1971**, *229*, 100.
(33) Lumry, R. In *Bioenergetics and Thermodynamics: Model Systems*; Braibanti, A., Ed.; Reidel: Dordrecht, Holland, 1980; pp 405-427.